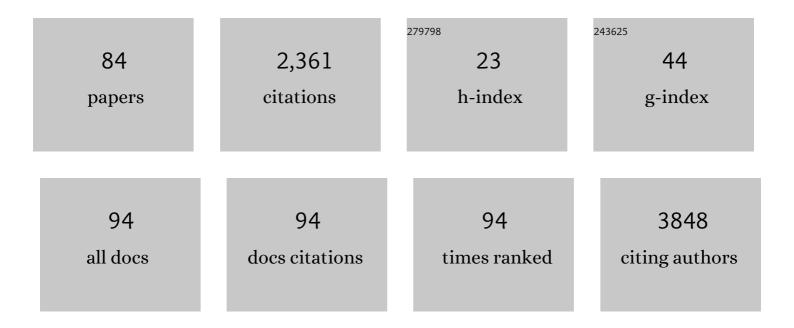
List of Publications by Year in descending order

Source: https://exaly.com/author-pdf/8850450/publications.pdf

Version: 2024-02-01



FRIC C ROUCHEA

#	Article	IF	CITATIONS
1	Enhancement of the gut barrier integrity by a microbial metabolite through the Nrf2 pathway. Nature Communications, 2019, 10, 89.	12.8	420
2	Gibbs Recursive Sampler: finding transcription factor binding sites. Nucleic Acids Research, 2003, 31, 3580-3585.	14.5	261
3	A Critical Role of the IL-1β–IL-1R Signaling Pathway in Skin Inflammation and Psoriasis Pathogenesis. Journal of Investigative Dermatology, 2019, 139, 146-156.	0.7	152
4	Transcription factor c-Maf is a checkpoint that programs macrophages in lung cancer. Journal of Clinical Investigation, 2020, 130, 2081-2096.	8.2	108
5	A specific low-density neutrophil population correlates with hypercoagulation and disease severity in hospitalized COVID-19 patients. JCI Insight, 2021, 6, .	5.0	79
6	HNRNPA2/B1 is upregulated in endocrine-resistant LCC9 breast cancer cells and alters the miRNA transcriptome when overexpressed in MCF-7 cells. Scientific Reports, 2019, 9, 9430.	3.3	78
7	Involvement of PARP1 in the regulation of alternative splicing. Cell Discovery, 2016, 2, 15046.	6.7	63
8	A comparison of per sample global scaling and per gene normalization methods for differential expression analysis of RNA-seq data. PLoS ONE, 2017, 12, e0176185.	2.5	60
9	Genome-Wide Profiling of PARP1 Reveals an Interplay with Gene Regulatory Regions and DNA Methylation. PLoS ONE, 2015, 10, e0135410.	2.5	55
10	rMAPS: RNA map analysis and plotting server for alternative exon regulation. Nucleic Acids Research, 2016, 44, W333-W338.	14.5	54
11	Transcriptome-wide identification of the RNA-binding landscape of the chromatin-associated protein PARP1 reveals functions in RNA biogenesis. Cell Discovery, 2017, 3, 17043.	6.7	50
12	Inorganic Arsenic-induced cellular transformation is coupled with genome wide changes in chromatin structure, transcriptome and splicing patterns. BMC Genomics, 2015, 16, 212.	2.8	43
13	Decreased ω-6:ω-3 PUFA ratio attenuates ethanol-induced alterations in intestinal homeostasis, microbiota, and liver injury. Journal of Lipid Research, 2019, 60, 2034-2049.	4.2	39
14	Coupling of PARP1-mediated chromatin structural changes to transcriptional RNA polymerase II elongation and cotranscriptional splicing. Epigenetics and Chromatin, 2019, 12, 15.	3.9	39
15	rMAPS2: an update of the RNA map analysis and plotting server for alternative splicing regulation. Nucleic Acids Research, 2020, 48, W300-W306.	14.5	39
16	Polystyrene bead ingestion promotes adiposity and cardiometabolic disease in mice. Ecotoxicology and Environmental Safety, 2022, 232, 113239.	6.0	33
17	Transcriptomic response of breast cancer cells to anacardic acid. Scientific Reports, 2018, 8, 8063.	3.3	32
18	Variant analysis of 1,040 SARS-CoV-2 genomes. PLoS ONE, 2020, 15, e0241535.	2.5	32

#	Article	IF	CITATIONS
19	Nuclear respiratory factor-1 and bioenergetics in tamoxifen-resistant breast cancer cells. Experimental Cell Research, 2016, 347, 222-231.	2.6	30
20	The induction of peripheral trained immunity in the pancreas incites anti-tumor activity to control pancreatic cancer progression. Nature Communications, 2022, 13, 759.	12.8	30
21	categoryCompare, an analytical tool based on feature annotations. Frontiers in Genetics, 2014, 5, 98.	2.3	29
22	<i>Yersinia pestis</i> Targets the Host Endosome Recycling Pathway during the Biogenesis of the <i>Yersinia</i> -Containing Vacuole To Avoid Killing by Macrophages. MBio, 2018, 9, .	4.1	29
23	Choice of library size normalization and statistical methods for differential gene expression analysis in balanced two-group comparisons for RNA-seq studies. BMC Genomics, 2020, 21, 75.	2.8	29
24	Identification of successful mentoring communities using network-based analysis of mentor–mentee relationships across Nobel laureates. Scientometrics, 2017, 111, 1733-1749.	3.0	28
25	The Adaptor Protein CD2AP Is a Coordinator of Neurotrophin Signaling-Mediated Axon Arbor Plasticity. Journal of Neuroscience, 2016, 36, 4259-4275.	3.6	27
26	Identification of a plasma metabolomic signature of thrombotic myocardial infarction that is distinct from non-thrombotic myocardial infarction and stable coronary artery disease. PLoS ONE, 2017, 12, e0175591.	2.5	27
27	DNA motif detection using particle swarm optimization and expectation-maximization. , 2005, 2005, 181-184.		23
28	Identification of G-quadruplex forming sequences in three manatee papillomaviruses. PLoS ONE, 2018, 13, e0195625.	2.5	22
29	Leukotriene B4-receptor-1 mediated host response shapes gut microbiota and controls colon tumor progression. Oncolmmunology, 2017, 6, e1361593.	4.6	20
30	Improved locomotor recovery after contusive spinal cord injury in Bmal1â^'/â^' mice is associated with protection of the blood spinal cord barrier. Scientific Reports, 2020, 10, 14212.	3.3	20
31	MPrime: efficient large scale multiple primer and oligonucleotide design for customized gene microarrays. BMC Bioinformatics, 2005, 6, 175.	2.6	19
32	IB4â€binding sensory neurons in the adult rat express a novel 3′ UTRâ€extended isoform of <i>CaMK4</i> that is associated with its localization to axons. Journal of Comparative Neurology, 2014, 522, 308-336.	1.6	17
33	Transcriptomic analysis of immune response to bacterial lipopolysaccharide in zebra finch (Taeniopygia guttata). BMC Genomics, 2019, 20, 647.	2.8	17
34	Computational Analysis of G-Quadruplex Forming Sequences across Chromosomes Reveals High Density Patterns Near the Terminal Ends. PLoS ONE, 2016, 11, e0165101.	2.5	16
35	Systems characterization of differential plasma metabolome perturbations following thrombotic and non-thrombotic myocardial infarction. Journal of Proteomics, 2017, 160, 38-46.	2.4	15
36	Induction of interferon response by high viral loads at early stage infection may protect against severe outcomes in COVID-19 patients. Scientific Reports, 2021, 11, 15715.	3.3	15

#	Article	IF	CITATIONS
37	The Rapid Assessment of Aggregated Wastewater Samples for Genomic Surveillance of SARS-CoV-2 on a City-Wide Scale. Pathogens, 2021, 10, 1271.	2.8	15
38	Transcriptional changes in sensory ganglia associated with primary afferent axon collateral sprouting in spared dermatome model. Genomics Data, 2015, 6, 249-252.	1.3	14
39	Dynamic trafficking patterns of IL-17-producing γδT cells are linked to the recurrence of skin inflammation in psoriasis-like dermatitis. EBioMedicine, 2022, 82, 104136.	6.1	14
40	rMotifGen: random motif generator for DNA and protein sequences. BMC Bioinformatics, 2007, 8, 292.	2.6	13
41	Shoc2-tranduced ERK1/2 motility signals — Novel insights from functional genomics. Cellular Signalling, 2016, 28, 448-459.	3.6	13
42	Whole Transcriptome Analysis Reveals That Filifactor alocis Modulates TNFα-Stimulated MAPK Activation in Human Neutrophils. Frontiers in Immunology, 2020, 11, 497.	4.8	13
43	Genome-wide miRNA response to anacardic acid in breast cancer cells. PLoS ONE, 2017, 12, e0184471.	2.5	13
44	Effect of single nucleotide polymorphisms on Affymetrix® match-mismatch probe pairs. Bioinformation, 2008, 2, 405-411.	0.5	13
45	RBF-TSS: Identification of Transcription Start Site in Human Using Radial Basis Functions Network and Oligonucleotide Positional Frequencies. PLoS ONE, 2009, 4, e4878.	2.5	12
46	Transcription Factor STAT3 Serves as a Negative Regulator Controlling IgE Class Switching in Mice. ImmunoHorizons, 2018, 2, 349-362.	1.8	12
47	Discovery of a Family of Genomic Sequences Which Interact Specifically with the c-MYC Promoter to Regulate c-MYC Expression. PLoS ONE, 2016, 11, e0161588.	2.5	11
48	Detection of Differentially Expressed Cleavage Site Intervals Within 3′ Untranslated Regions Using CSI-UTR Reveals Regulated Interaction Motifs. Frontiers in Genetics, 2019, 10, 182.	2.3	11
49	DNA-based random number generation in security circuitry. BioSystems, 2010, 100, 208-214.	2.0	10
50	Framework for reanalysis of publicly available Affymetrix® GeneChip® data sets based on functional regions of interest. BMC Genomics, 2017, 18, 875.	2.8	10
51	Activity/exercise-induced changes in the liver transcriptome after chronic spinal cord injury. Scientific Data, 2019, 6, 88.	5.3	9
52	Comparative gene expression analysis in melanocytes driven by tumor cell-derived exosomes. Experimental Cell Research, 2020, 386, 111690.	2.6	9
53	Glial granules contain germline proteins in the Drosophila brain, which regulate brain transcriptome. Communications Biology, 2020, 3, 699.	4.4	9
54	DNA media storage. Progress in Natural Science: Materials International, 2008, 18, 603-609.	4.4	8

#	Article	IF	CITATIONS
55	Transcriptional profile of immediate response to ionizing radiation exposure. Genomics Data, 2016, 7, 82-85.	1.3	8
56	Regulation of miR-29b-1/a transcription and identification of target mRNAs in CHO-K1 cells. Molecular and Cellular Endocrinology, 2017, 444, 38-47.	3.2	8
57	Transcriptome of dorsal root ganglia caudal to a spinal cord injury with modulated behavioral activity. Scientific Data, 2019, 6, 83.	5.3	7
58	Multiomics analysis of the impact of polychlorinated biphenyls on environmental liver disease in a mouse model. Environmental Toxicology and Pharmacology, 2022, 94, 103928.	4.0	7
59	Detecting and accounting for multiple sources of positional variance in peak list registration analysis and spin system grouping. Journal of Biomolecular NMR, 2017, 68, 281-296.	2.8	6
60	<i>Pas de deux</i> : An Intricate Dance of Anther Smut and Its Host. G3: Genes, Genomes, Genetics, 2018, 8, 505-518.	1.8	6
61	A combined approach with gene-wise normalization improves the analysis of RNA-seq data in human breast cancer subtypes. PLoS ONE, 2018, 13, e0201813.	2.5	6
62	Dataset for dose and time-dependent transcriptional response to ionizing radiation exposure. Data in Brief, 2019, 27, 104624.	1.0	5
63	lleum Gene Expression in Response to Acute Systemic Inflammation in Mice Chronically Fed Ethanol: Beneficial Effects of Elevated Tissue n-3 PUFAs. International Journal of Molecular Sciences, 2021, 22, 1582.	4.1	5
64	Exposure to Fine Particulate Matter Air Pollution Alters mRNA and miRNA Expression in Bone Marrow-Derived Endothelial Progenitor Cells from Mice. Genes, 2021, 12, 1058.	2.4	5
65	Database of exact tandem repeats in the Zebrafish genome. BMC Genomics, 2010, 11, 347.	2.8	4
66	DNA-based dynamic logic circuitry. , 2010, , .		4
67	Data set for transcriptional response to depletion of the Shoc2 scaffolding protein. Data in Brief, 2016, 7, 770-778.	1.0	4
68	Feature Selection in Cancer Classification from mRNA Data Based on Localized Dimension Reduction. , 2009, , .		3
69	Transcriptional signatures of the small intestinal mucosa in response to ethanol in transgenic mice rich in endogenous n3 fatty acids. Scientific Reports, 2020, 10, 19930.	3.3	3
70	Affymetrix® Mismatch (MM) Probes: Useful after All. , 2012, , .		2
71	Adjusted Sample Size Calculation for RNA-seq Data in the Presence of Confounding Covariates. BioMedInformatics, 2021, 1, 47-63.	2.0	2
72	Computational Prediction of Genes Translationally Regulated by Cytoplasmic Polyadenylation Elements. Lecture Notes in Computer Science, 2009, , 353-361.	1.3	2

#	Article	IF	CITATIONS
73	Inference and Sample Size Calculations Based on Statistical Tests in a Negative Binomial Distribution for Differential Gene Expression in RNAseq Data. Journal of Biometrics & Biostatistics, 2017, 08, .	4.0	2
74	Interval Trees for Detection of Overlapping Genetic Entities. , 2011, , .		1
75	An Island-Based Approach for Differential Expression Analysis. , 2013, 2013, 419-429.		1
76	RNA-seq data of soleus muscle tissue after spinal cord injury under conditions of inactivity and applied exercise. Data in Brief, 2020, 28, 105056.	1.0	1
77	Sex-Based Differences in Cardiac Gene Expression and Function in BDNF Val66Met Mice. International Journal of Molecular Sciences, 2021, 22, 7002.	4.1	1
78	Combined exposure to polychlorinated biphenyls and high-fat diet modifies the global epitranscriptomic landscape in mouse liver. Environmental Epigenetics, 2021, 7, dvab008.	1.8	1
79	A Heuristic Algorithm for Detecting Intercellular Interactions. , 2011, , .		0
80	A comparison of combined p-value methods for gene differential expression using RNA-seq data. , 2014, , ,		0
81	Region-based custom chip description formats for reanalysis of publicly available affymetrix $\hat{A}^{0}$ genechip $\hat{A}^{0}$ data sets. , 2016, , .		0
82	Cover Image, Volume 85, Issue 5. Proteins: Structure, Function and Bioinformatics, 2017, 85, C1-C1.	2.6	0
83	Dietary copperâ€fructose interactions alter gut microbiome in a sexâ€differential manner likely contributes to the sex differences in the metabolic phenotype. FASEB Journal, 2020, 34, 1-1.	0.5	0
84	Differential Expression of Long Noncoding RNAs in Murine Myoblasts After Short Hairpin RNA-Mediated Dysferlin Silencing In Vitro: Microarray Profiling. JMIR Bioinformatics and Biotechnology, 2022, 3, e33186.	0.9	0